Contrib. Astron. Obs. Skalnaté Pleso **33**, 224 – 232, (2003)

# The range of reliability of the line-of-sight velocity in a semiempirical model of a granule

**J. Koza and A. Kučera**

*Astronomical Institute of the Slovak Academy of Sciences*
*059 60 Tatranská Lomnica, The Slovak Republic, (E-mail: koza@astro.sk)*

Received: May 26, 2003

**Abstract.** Stokes $I$ response functions to the line-of-sight velocity $v_{\rm LOS}$ of two medium-strong Fe I 522.5 nm and Fe I 557.6 nm lines and the weak line Fe I 557.7 nm have been calculated using a semiempirical 1D model of the granular photosphere affected by 5-min oscillations. A new method is presented allowing to estimate the range of optical depths within which the inferred values of an atmospheric parameter can be considered as reliable. The sensitivity of the individual lines to the variations of $v_{\rm LOS}$ is examined and the range of reliability of $v_{\rm LOS}$ is estimated applying the new method. It is shown that for the given line set the Fe I 522.5 nm line is the most sensitive one and, in turn, the Fe I 557.7 nm line has very low sensitivity to the variations of $v_{\rm LOS}$. In the case of the Fe I 522.5 nm line the impact of a $v_{\rm LOS}$ perturbation on the intensity of a profile point is about 50% greater than that on the Fe I 557.6 nm line. As a consequence of evolution of the physical conditions in a granule the range of reliability of the model varies and it consists of two separate regions occupying the lower and upper photosphere.

**Key words:** line: formation – radiation transfer – Sun: photosphere – granulation – stars: atmospheres

## 1. Introduction

A perturbation analysis of the radiative transfer equation yields a particular class of functions enabling us to inspect the sensitivity of the spectral line intensity to small variations of either atomic line parameters or atmospheric parameters. These so-called response functions (RFs) became a cornerstone of the inversion code 'SIR', which is the acronym of Stokes Inversion based on Response functions (Ruiz Cobo, del Toro Iniesta 1992). The SIR code gives a possibility to translate an observed spectrum into physical quantities, or in turn, to calculate the synthetic line profiles and the RFs for a given atmospheric model. Applying the SIR code to the time series of high resolution solar photospheric spectra the temporal evolution of physical parameters in a granule was obtained (Koza *et al.*, 2002; Koza *et al.*, 2003). Using this model and the SIR code we calculated the set of RFs to $v_{\rm LOS}$ for three iron lines. If a specific assumption is fulfilled then the RFs may be used for an estimate of the range of optical depths within which the relevant atmospheric parameter is known reliably enough. The present work is devoted to a practical application of this idea.

## 2. Response functions – general characteristics

Because of intricate non-linear dependence of the spectrum on various atomic and atmospheric parameters, the family of RFs is numerous. There are two distinct groups: the RFs to atomic parameters and the RFs to atmospheric parameters (Ruiz Cobo, del Toro Iniesta 1994). A brief overview of their common characteristics follows:

– the RFs contain information about how the spectrum responds to small modifications of physical parameters,

– the RFs behave like partial derivatives of the spectrum with respect to the relevant physical parameters involved in the LTE line formation,

– the RFs are bivariate functions of some spatial coordinate (usually optical depth) and wavelength,

– the RFs are model and line dependent,

– the RFs vary strongly across the wavelength span of a given line and also across the spatial grid of a model.

Finally, the presence of the line-of-sight velocity gradient in the model breaks down the symmetry of the Stokes $I$ RFs to temperature with respect to the line centre (Koza, Kučera 2002).

## 3. Range of reliability – concept definition

Generally, the reliability of the results inferred by the SIR code is limited to those layers from which physical information is available, i.e. to those layers in which the RFs are significantly different from zero (del Toro Iniesta, 1996). Thus, adopting certain assumptions, the RFs allow to estimate the reliability of the results. Let us try to expand this idea putting it on a firm ground by a more stringent definition.

Let $x_j(\tau)$, $j = 1, 2, \ldots, m$, be the set of physical quantities characterizing an atmospheric model. For example, $x_1$ denotes the temperature, $x_2$ the line-of-sight velocity, $x_3$ microturbulence, etc. It can be proven (del Toro Iniesta, 2001) that small perturbations $\delta x_j(\tau)$ of these quantities induce small modifications $\delta I(\lambda)$ to the line profile intensity at wavelength $\lambda$. A modification $\delta I(\lambda)$ can be written as:

$$\delta I(\lambda) = \sum_{j=1}^{m} \int_0^\infty R_j(\tau,\, \lambda)\, \delta x_j(\tau) \mathrm{d}\tau, \tag{1}$$

where $\tau$ represents the continuum optical depth at 500 nm and $R_j(\tau, \lambda)$ is the response function for the atmospheric parameter $x_j$. Let $\delta x_j(\tau)$ be the impulse perturbation defined as:

$$\delta x_j(\tau) = A\delta(\tau - \tau_0), \tag{2}$$

where the amplitude $A$ is a non-zero constant of the same unit as the parameter $x_j$. It is identified with the standard deviation of the errors resulting from the inversion of the parameter, $\delta(\tau - \tau_0)$ is Dirac's delta function and $\tau_0 \in \langle\tau_1, \tau_2\rangle$. Combining Eqs. 1 and 2 for the fixed index $j$ (i.e. for the selected atmospheric parameter) we can write:

$$\delta I(\lambda) = AR_j(\tau_0, \lambda). \tag{3}$$

Now suppose that the synthetic line intensities $I_\mathrm{s}$ resulting from the inversion fit the observed intensities $I_\mathrm{o}$ within the limits of the observational uncertainty $\varepsilon$ within the whole wavelength range of a line profile, so that $|I_\mathrm{s} - I_\mathrm{o}| \leq \varepsilon$. If the set $\langle\tau_1, \tau_2\rangle$ contains all optical depths for which it is valid that the impulse perturbation of the final model induces the misfit $\delta I(\lambda)$ exceeding the observational uncertainty such that $|\delta I| > \varepsilon$, then the set $\langle\tau_1, \tau_2\rangle$ will be called *the range of reliability* of the atmospheric parameter $x_j$. Using the latter inequality and Eq. 3, one obtains:

$$|R_j(\tau_0, \lambda)| > \frac{\varepsilon}{|A|}\ . \tag{4}$$

The inequality 4 suggests that the absolute value of the response function calculated within the range of reliability exceeds a certain limit. It exactly defines which values of the response function are significantly different from zero with respect to the adopted assumptions. This is fundamental for our further consideration because inequality 4 enables us to estimate the range of reliability which is *a priori* unknown. The following procedure outlines how to localize this range:

1. calculation of the set of RFs to the atmospheric parameter $x_j$ for all spectral lines involved in the inversion using the final model.

2. estimate of the observational uncertainty $\varepsilon$ and calculation of the amplitude $A$. The latter may also be estimated if some relevant facts are taken into account.

3. estimate of the ranges of reliability applying inequality 4 to the RFs calculated in step 1. The optical depths, within which inequality 4 is valid, are determined.

4. unification in the mathematical sense of all individual ranges determined in step 3. The result is the range of reliability of the atmospheric parameter.

5. dealing with temporal evolution steps 1, 3 and 4 are repeated for every instantaneous model. In this way the time dependence of the range of reliability is obtained.

Intentionally, following the aim of this paper, we will henceforth deal only with the RFs to the line-of-sight velocity .

## 4. Stokes $I$ response function to line-of-sight velocity

In LTE the Stokes $I$ response function to a perturbation of the line-of-sight velocity $\mathcal{R}_{\rm V}$ is defined as:

$$\mathcal{R}_{\rm V}(\tau,\,\lambda) = \frac{{\rm e}^{-\tau_\lambda}}{\alpha(\tau)}\frac{\partial\alpha_\lambda(\tau)}{\partial v_{\rm LOS}}\left[B_\lambda(\tau) - I_\lambda(\tau)\right], \tag{5}$$

where $\alpha(\tau)$ and $\alpha_\lambda(\tau)$ are the extinction coefficients at the continuum at 500 nm and at a given wavelength $\lambda$, respectively, $B_\lambda(\tau)$ is the Planck function, $I_\lambda(\tau)$ is the monochromatic intensity, e is the Euler number 2.71828... and $\tau_\lambda$ is the optical depth at a given wavelength $\lambda$ calculated from:

$$\tau_\lambda = \int\limits_0^\tau \frac{\alpha_\lambda}{\alpha}{\rm d}\tau\ . \tag{6}$$

A detailed derivation of Eq. 5 in a generalized vector form can be found in del Toro Iniesta (2001). The effect of macroturbulence is simulated by convolving $\mathcal{R}_{\rm V}(\tau,\,\lambda)$ with the Gaussian $M$:

$$M(\lambda-\lambda_0, v_{\rm mac}) = \frac{1}{\sqrt{2\pi}\;\sigma}{\rm e}^{-\frac{(\lambda-\lambda_0)^2}{2\sigma^2}}, \tag{7}$$

where $\sigma \equiv \lambda_0 v_{\rm mac}/{\rm c}$, $\lambda_0$ is the central wavelength of the transition, $v_{\rm mac}$ is the macroturbulent velocity and c is the speed of light. The convolution may be written as:

$$\mathcal{R}^*_{\rm V}(\tau,\,\lambda) = M(\lambda) * \mathcal{R}_{\rm V}(\tau,\,\lambda). \tag{8}$$

As the depth scale the logarithm of the continuum optical depth $\log\tau$ at 500 nm will be used hereafter. Moreover, the discretization of the atmospheric model is needed for numerical calculations. Thus introducing into Eqs. 5 and 8 a $\log\tau$ scale and discretization, one gets:

$$R^*_{\rm V}(\log\tau_i,\,\lambda) = \mathcal{R}^*_{\rm V}(\tau_i,\,\lambda)\tau_i\ln 10. \tag{9}$$

The index $i = 1,\ldots,{\rm N}$ samples the individual layers of the atmosphere used as an input for the SIR code. The resulting $R^*_{\rm V}$ are absolute RFs in contrast to relative RFs (Ruiz Cobo, del Toro Iniesta 1994), thus their unit is $({\rm cm\,s^{-1}})^{-1}$. The energy unit is omitted because of normalization of the $R^*_{\rm V}$ to the HSRA continuum intensity at the disk centre at the central wavelength of a given line. All the mentioned formulae are implemented in the SIR code.

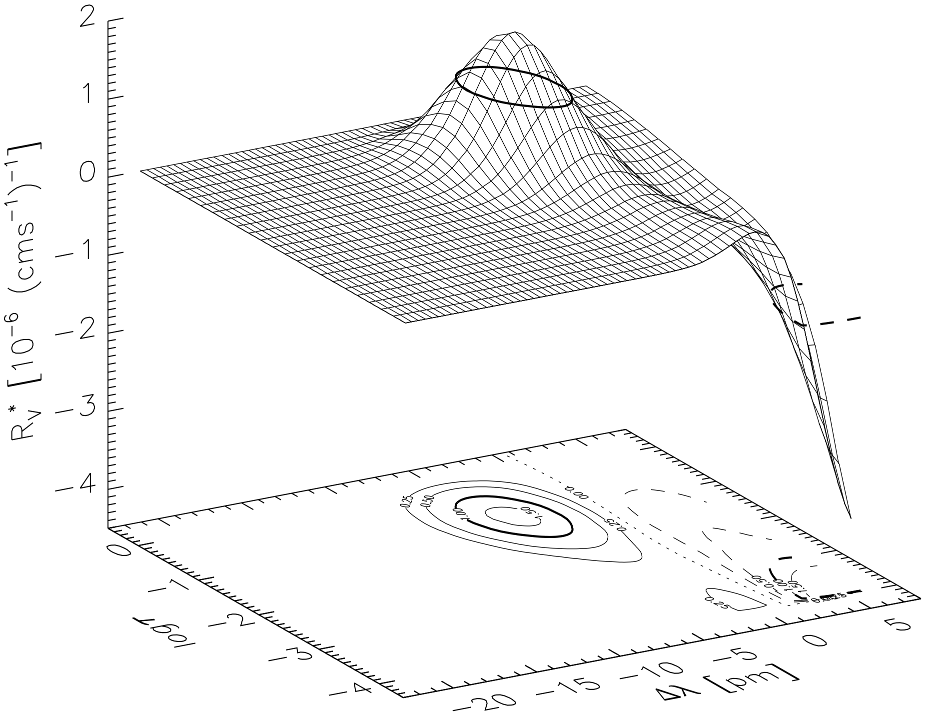


**Figure 1.** The absolute Stokes $I$ response function to the line-of-sight velocity $R^*_{\rm V}$ of the Fe I 522.5 nm line normalized to the HSRA continuum at the disk centre at the central wavelength of the line. The model representing the physical conditions in the centre of the granule at $t = 0$ min was used in the calculation. The value of 0 pm corresponds to the laboratory wavelength of the line. The solid and dashed contour lines are projection of some positive and negative values of $R^*_{\rm V}$ respectively to $(\log\tau, \Delta\lambda)$ plane. The contours of 0.0 (dotted), $\pm\,0.25$, $\pm\,0.50$, $\pm\,1.00$ and $\pm\,1.50 \times 10^{-6}\,({\rm cm\,s^{-1}})^{-1}$ are explicitly depicted.

## 5. Calculations and results

In our previous work (Koza *et al.*, 2002; Koza *et al.*, 2003) the time series of spectra containing the profiles of Fe I 522.5 nm, Fe I 557.6 nm and Fe I 557.7 nm lines were inverted by the SIR code. The profiles originated from the center of a bright granule. As far as we know, in this way the temporal evolution of the

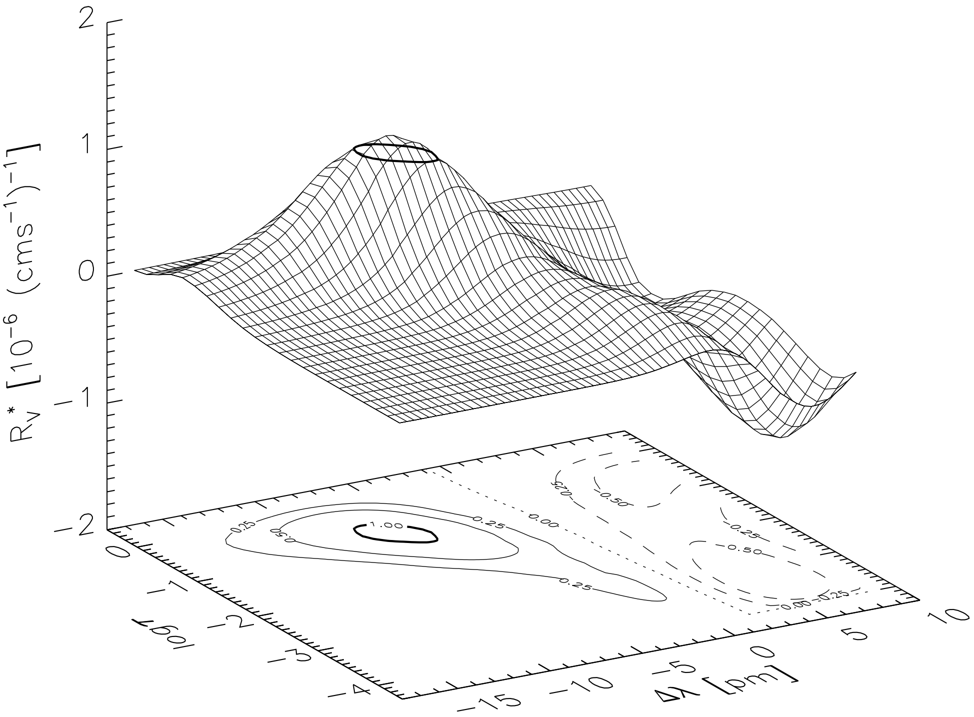


**Figure 2.** Same as in Fig. 1 but for the Fe I 557.6 nm line.

temperature and line-of-sight velocity in the granule center were obtained for the first time. Now the range of reliability of the line-of-sight velocity in these models is going to be subject of examination applying the procedure described in section 3. The value of $1 \times 10^{-2}$ was found for the observational uncertainty.

Instead of a standard deviation of the errors of $v_{\mathrm{LOS}}$ the value of $100\,\mathrm{m\,s^{-1}}$ was adopted for the amplitude $A$ as typical errors of the solar and laboratory wavelengths of the lines used for wavelength scale calibration and inversion of the spectra. Thus the limiting absolute value of $R_{\mathrm{V}}^*$ is $1 \times 10^{-6}\,(\mathrm{cm\,s^{-1}})^{-1}$ (see inequality 4). Applying Eq. 9 the set of $R_{\mathrm{V}}^*$ was calculated for Fe I 522.5 nm, Fe I 557.6 nm and Fe I 557.7 nm lines, examples of which are shown in Figs. 1, 2 and 3. There are also highlighted thick contours helping to identify the limits within which the absolute value of $R_{\mathrm{V}}^*$ is greater than $1 \times 10^{-6}\,(\mathrm{cm\,s^{-1}})^{-1}$ in these particular cases. At first glance, the following features of $R_{\mathrm{V}}^*$ are obvious:

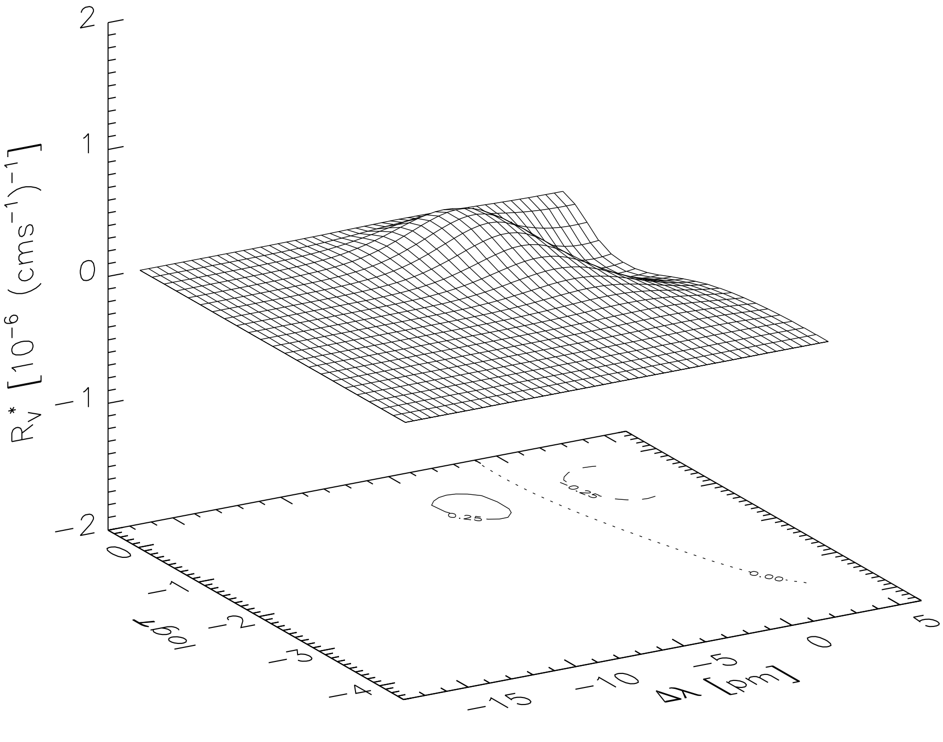


**Figure 3.** Same as in Fig. 1 but for the Fe I 557.7 nm line.

- the $R_V^*$ are asymmetric with respect to the line centre,
- the $R_V^*$ change sign,
- in case of the Fe I 522.5 nm and Fe I 557.6 nm lines the blue and red lobes of the $R_V^*$ probe the lower and upper photosphere, respectively, whereas the $R_V^*$ of the weak Fe I 557.7 nm line carries information only about the lower photosphere,
- the local maxima of the $R_V^*$ occur at the wavelengths corresponding to the line wings.

These features are common for the whole set of $R_V^*$. Fig. 4 depicts cuts of $R_V^*$ shown in Figs. 1, 2 and 3 at the estimated wavelengths of the local maxima. Clearly, the Fe I 522.5 nm line is most sensitive to the perturbations of $v_{LOS}$.

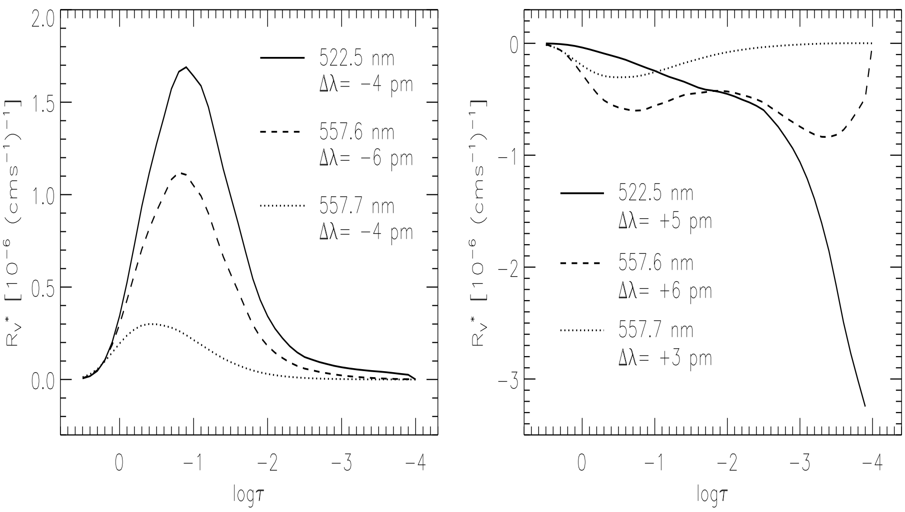


**Figure 4.** The cuts of Stokes $I$ response functions to the line-of-sight velocity $R_{\mathrm{V}}^{*}$ shown in Figs. 1, 2 and 3 at indicated $\Delta\lambda$ from the line centre.

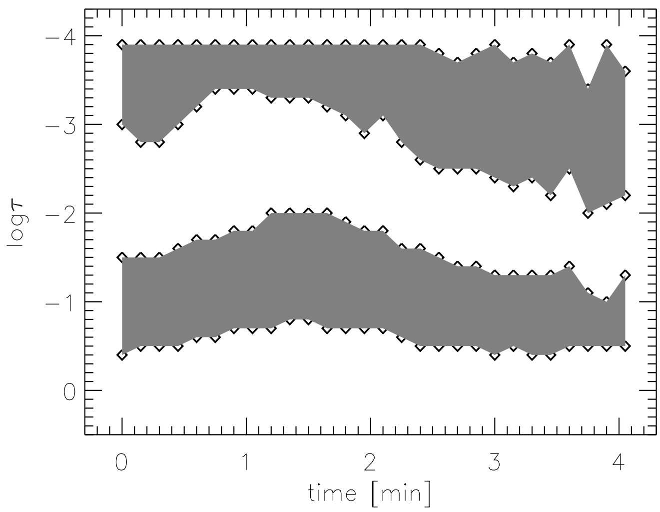


**Figure 5.** The ranges of reliability (shaded areas) of the line-of-sight velocity in the semiempirical model of a granule. The time dependence represents different moments of the observations, i.e. the evolution of the physical conditions in the centre of the granule. Following item 4 in section 3, the ranges are a unification of the particular subranges corresponding to the lines we are dealing with (i.e. Fe I 522.5 nm, Fe I 557.6 nm and Fe I 557.7 nm). In fact, the shape and extent of the shaded area is fully determined by the $R_{\mathrm{V}}^{*}$ of the Fe I 522.5 nm line as the line with the broadest subranges of reliability.

Finally, applying inequality 4 to the whole set of $R^*_{\mathrm{V}}$ computed for all investigated lines the time dependence of the ranges of reliability was obtained, which is shown in Fig. 5. Due to the presence of two distinct lobes in the shape of $R^*_{\mathrm{V}}$ the ranges of reliability are separated into two subregions. The positions of the borders, as well as the extent of them, vary in time as a consequence of the evolution of the physical parameters in a granule.

## 6. Discussion and conclusion

This paper aims at introducing a new method for an estimate of the ranges of reliability of the models inferred by the SIR code. We also focus on qualitative characteristics of Stokes $I$ RFs to the perturbations of the line-of-sight velocity $R^*_{\mathrm{V}}$ calculated by means of the models of the granular photosphere affected by 5-min oscillations. The velocity gradients involved in the models (see Figs. 1 and 2 in Koza *et al.*, 2002) induce a strong asymmetry of the $R^*_{\mathrm{V}}$ with respect to the line centre, as it can be seen in Figs. 1 and 2. Moreover, the isolated peaks of sensitivity occur in the $R^*_{\mathrm{V}}$. This suggests a remarkable relation between the layers affected by some hypothetical perturbation of $v_{\mathrm{LOS}}$ and the corresponding line profile variation. The lower located peaks ($\log\tau \sim -1, \Delta\lambda \sim -5\,\mathrm{pm}$) imply that some hypothetical perturbations of $v_{\mathrm{LOS}}$ in the lower layers influence predominately the blue line wings. In turn, the upper located peaks ($\log\tau \sim -3, \Delta\lambda \sim +5\,\mathrm{pm}$) cause that perturbations of $v_{\mathrm{LOS}}$ in these layers affect the red wings. The separation of the ranges of reliability into two subregions is a direct consequence of the presence of two isolated peaks of sensitivity in $R^*_{\mathrm{V}}$ (see Fig. 5). We can conclude that the medium-strong photospheric lines supply reliable information about velocities in the lower as well as uppermost photospheric layers. Finally, the velocity inferred by the SIR code should be reliable in a wide but not continuous range of optical depths.

**Acknowledgements.** GA SAV (grant VEGA 2/3015/23) supported this work.

## References

Koza, J., Bellot Rubio, L.R., Kučera, A., Hanslmeier, A., Rybák, J., Wöhl, H.: 2002, in *Solar Variability: From Core to Outer Frontiers*, ed.: A. Wilson, ESA SP-506, Noordwijk, 443

Koza, J., Bellot Rubio, L.R., Kučera, A., Hanslmeier, A., Rybák, J., Wöhl, H.: 2003, *Astron. Nachr.* **324**, No. 4, 349

Koza, J., Kučera, A.: 2002, *Contrib. Astron. Obs. Skalnaté Pleso* **32**, 190

Ruiz Cobo, B., del Toro Iniesta, J.C.: 1992, *Astrophys. J.* **398**, 375

Ruiz Cobo, B., del Toro Iniesta, J.C.: 1994, *Astron. Astrophys.* **283**, 129

del Toro Iniesta, J.C., Ruiz Cobo, B.: 1996, *Sol. Phys.* **164**, 169

del Toro Iniesta, J.C.: 2001, in *The Dynamic Sun*, eds.: A. Hanslmeier, M. Messerotti and A. Veronig, Kluwer Academic Publishers, Dordrecht, 183